

MHD boundary-layer flow due to a moving extensible surface

Anuar Ishak · Roslinda Nazar · Ioan Pop

Received: 26 October 2006 / Accepted: 5 July 2007 / Published online: 4 August 2007
© Springer Science+Business Media B.V. 2007

Abstract The flow due to a moving extensible sheet that obeys a more general stretching law is considered. The sheet occupies the negative x -axis and is moving continually in the positive x -direction, in an incompressible viscous and electrically conducting fluid. The sheet somehow disappears in a sink that is located at $(x, y) = (0, 0)$. The governing system of partial differential equations is first transformed into a system of ordinary differential equations, and the transformed equations are solved numerically using a finite-difference scheme, namely the Keller-box method. The features of the flow and heat-transfer characteristics for different values of the governing parameters are analyzed and discussed. It is found that dual solutions exist for the flow near $x = 0$, where the velocity profiles show a reversed flow.

Keywords Boundary layer · Dual solutions · Magnetohydrodynamic (MHD) · Similarity solution · Stretching sheet

1 Introduction

The study of the flow field due to a stretching surface in a quiescent or moving fluid is relevant to several practical applications in modern industry. A few practical examples include industrial processes such as the extrusion of metals and plastics, cooling and/or drying of papers and textiles, glass blowing and material handling which involve boundary layers on continuous moving surfaces in a free stream under significant boundary conditions. It must, however, be pointed out that the problem of boundary-layer flow adjacent to a continuous moving sheet is physically different from that of the classical Blasius flow past a stationary flat plate and that the two problems cannot be mathematically transformed from one to the other. It seems that Sakiadis [1, 2] was the first to analyze the boundary layer on continuous semi-infinite sheets and cylindrical rods moving steadily in an otherwise quiescent environment. Subsequently, several investigators [3–8] have studied various aspects of this problem such as the effect of the mass transfer, wall temperature and magnetic field. The study of magnetohydrodynamic (MHD) flow of an electrically conducting fluid caused by the deformation of the walls of the vessel containing this fluid is of considerable interest

A. Ishak · R. Nazar
School of Mathematical Sciences, Universiti Kebangsaan Malaysia, 43600 UKM Bangi, Selangor, Malaysia

I. Pop (✉)
Faculty of Mathematics, University of Cluj, CP 253, Cluj 3400, Romania
e-mail: pop.ioan@yahoo.co.uk

in modern metallurgical and metal-working processes. In all these cases, the quality of the final product depends on the rate of heat transfer at the stretching surface. Crane [9] presented a similarity solution in closed analytical form for steady two-dimensional incompressible boundary-layer flow over a surface which is stretched in its own plane with a velocity varying linearly with the distance from a fixed point. Banks [10] considered a surface that is stretched with a velocity proportional to x^m , where x is the distance along the surface measured from a fixed point and m is a constant. Magyari and Keller [11, 12], and Magyari et al. [13] considered the case when the mass transfer (suction or injection) is proportional to a power of the distance x and presented very interesting closed-form analytical solutions. Carragher and Crane [14] gave a closed-form solution when the temperature difference between the stretched surface and the ambient fluid is proportional to x^n , where n is a constant. In a very interesting and original paper, Kuiken [15] has considered the boundary-layer flow due to a moving sheet that obeys a more general stretching law. The extensible sheet occupies the negative x -axis and is moving continually in the positive x -direction with a velocity

$$u_s(x) = (x_0/|x|)^n u_0, \quad (1)$$

where $n > 0$, x_0 is a characteristic length and u_0 is a characteristic velocity. It has been shown by Kuiken [15] that, if the Reynolds number $\text{Re} = u_0 x_0 / \nu$ is assumed to be large, a “backward” boundary layer exists along the moving sheet. The aim of this paper is to extend the paper by Kuiken [15] by considering the flow over a stretching sheet, which obeys Eq. 1 in an electrically conducting fluid, the flow being permeated by a variable transverse magnetic field. In addition, we will consider the case of heat transfer assuming that the surface is maintained at a variable wall temperature $T_w(x)$, which is proportional to $(x_0/|x|)^m$, where m is a positive constant.

2 Governing equations

Consider the steady two-dimensional flow of an incompressible viscous electrically conducting fluid caused by a stretching sheet, which is placed in an ambient fluid of uniform temperature T_∞ . We assume that the temperature of the sheet is $T_w(x)$ ($> T_\infty$), which corresponds to a heated sheet. We consider that a variable magnetic field $B(x)$ is applied normal to the sheet and that the induced magnetic field is neglected, which is justified for MHD flow at small magnetic Reynolds number, i.e., $\text{Re}_m = \mu_0 \sigma V L \ll 1$, where μ_0 is the magnetic permeability, σ is the electrical conductivity of the fluid, V is the characteristic velocity and L is the characteristic length scale of the problem considered (see [16]). It is also assumed that the external electric field is zero and the electric field due to polarization of charges is negligible. Under these assumptions, the MHD equations for the steady two-dimensional flow and heat transfer in the boundary layer over the stretching surface are

$$\frac{\partial u}{\partial x} + \frac{\partial v}{\partial y} = 0, \quad (2)$$

$$u \frac{\partial u}{\partial x} + v \frac{\partial u}{\partial y} = \nu \frac{\partial^2 u}{\partial y^2} - \frac{\sigma B^2(x)}{\rho} u, \quad (3)$$

$$u \frac{\partial T}{\partial x} + v \frac{\partial T}{\partial y} = \alpha \frac{\partial^2 T}{\partial y^2}, \quad (4)$$

where the y -axis is measured in the direction normal to the sheet, the flow being confined to $y > 0$, u and v are the velocity components along the x - and y -axes, respectively, T is the fluid temperature, α is the thermal diffusivity of the fluid and ρ is the density. We assume that the appropriate boundary conditions of Eqs. 2–4 are

$$\begin{aligned} u &= u_s(x), \quad v = 0, \quad T = T_w(x) \quad \text{at } y = 0, \\ u &\rightarrow 0, \quad T \rightarrow T_\infty \quad \text{as } y \rightarrow \infty, \end{aligned} \quad (5)$$

where $T_w(x) = T_\infty + T_0 (x_0/|x|)^m$ with T_0 as a characteristic temperature and $u_s(x)$ is as given in Eq. 1. The boundary conditions (5) must be completed with the conditions

$$u \rightarrow 0, \quad T \rightarrow T_\infty \quad \text{as } x \rightarrow -\infty. \quad (6)$$

To obtain similarity solutions, we assume that the magnetic field $B(x)$ be in the form (see [17–19])

$$B(x) = (x_0/|x|)^{(n+1)/2} B_0, \quad (7)$$

where B_0 is the constant magnetic field.

A little inspection shows that Eqs. 2–4, along with the boundary conditions (5) and (6), admit similarity solution by introducing the similarity variables of the form

$$\begin{aligned} \eta &= y \{u_s / (2\nu|x|)\}^{1/2}, \\ \psi &= (2\nu u_s |x|)^{1/2} f(\eta), \\ \theta(\eta) &= (T - T_\infty) / (T_w - T_\infty), \end{aligned} \quad (8)$$

where ψ is the stream function which is defined as $u = \partial\psi/\partial y$ and $v = -\partial\psi/\partial x$. Substituting (8) in Eqs. 2–4, we get the following ordinary differential equations:

$$f''' + (n-1)ff'' - 2nf'^2 - 2Mf' = 0, \quad (9)$$

$$\frac{1}{\text{Pr}}\theta'' + (n-1)f\theta' - 2mf'\theta = 0, \quad (10)$$

where $M = \sigma B_0^2 / (\rho u_0/x_0)$ is the magnetic parameter, Pr is the Prandtl number and primes denote differentiation with respect to η . The boundary conditions (5) become

$$\begin{aligned} f(0) &= 0, \quad f'(0) = 1, \quad \theta(0) = 1, \\ f'(\eta) &\rightarrow 0, \quad \theta(\eta) \rightarrow 0 \quad \text{as } \eta \rightarrow \infty. \end{aligned} \quad (11)$$

The physical quantities of interest are the skin friction coefficient C_f and the local Nusselt number Nu_x , which are defined by

$$C_f = \frac{\tau_w}{\rho u_s^2/2}, \quad \text{Nu}_x = \frac{xq_w}{k(T_w - T_\infty)}, \quad (12)$$

where the skin friction τ_w and the heat transfer from the surface q_w are given by

$$\tau_w = \mu \left(\frac{\partial u}{\partial y} \right)_{y=0}, \quad q_w = -k \left(\frac{\partial T}{\partial y} \right)_{y=0}, \quad (13)$$

with μ and k being the dynamic viscosity and thermal conductivity, respectively. Using the similarity variables (8), we get

$$\frac{1}{2}C_f \text{Re}_x^{1/2} = \frac{1}{\sqrt{2}}f''(0), \quad \text{Nu}_x/\text{Re}_x^{1/2} = -\frac{1}{\sqrt{2}}\theta'(0), \quad (14)$$

where $\text{Re}_x = u_s|x|/\nu$ is the local Reynolds number.

3 Numerical solution

3.1 Exact numerical solution

Equations 9 and 10 subject to the boundary conditions (11) are solved numerically using finite-difference approximations known as the Keller-box method, which is described in [20]. The solution is obtained in the following four steps:

- reduce Eqs. 9 and 10 to a first-order system;
- write the difference equations using central differences;
- linearize the resulting algebraic equations by Newton's method and write them in matrix-vector form;
- solve the linear system by the block-tridiagonal-elimination technique.

The step size of η , $\Delta\eta$, and the edge of the boundary layer, η_∞ , are adjusted for different range of parameters. To conserve space, the details of the solution procedure are not presented here.

3.2 Perturbation solution for small M

Following Ariel [21], we can get approximate solutions of Eqs. 9 and 10 subject to the boundary conditions (11) valid for small values of the magnetic parameter $M \ll 1$. By investigating the terms in the governing equation (9), we assume that the solution of Eqs. 9 and 10 for small $M (\ll 1)$ is of the form

$$f(\eta) = \sum_{i=0}^{\infty} f_i(\eta)M^i, \quad \theta(\eta) = \sum_{i=0}^{\infty} \theta_i(\eta)M^i, \quad (15)$$

where f_i and θ_i are the perturbations in f and θ , respectively. Substituting expressions (15) in Eqs. 9 and 10, and comparing like powers of M , we obtain the following set of equations:

$$f_0''' + (n-1)f_0f_0'' - 2nf_0'^2 = 0, \quad (16)$$

$$\frac{1}{\text{Pr}}\theta_0'' + (n-1)f_0\theta_0' - 2mf_0'\theta_0 = 0, \quad (17)$$

and

$$f_i''' + (n-1)\sum_{j=0}^i f_j f_{i-j}'' - 2n\sum_{j=0}^i f_j' f_{i-j}' - 2f_{i-1}' = 0, \quad (18)$$

$$\frac{1}{\text{Pr}}\theta_i'' + (n-1)\sum_{j=0}^i f_j \theta_{i-j}' - 2m\sum_{j=0}^i f_j' \theta_{i-j} = 0, \quad (19)$$

for $i \geq 1$, subject to boundary conditions

$$\begin{aligned} f_i(0) = 0, \quad f_i'(0) = \delta_{i0}, \quad \theta_i(0) = \delta_{i0}, \\ f_i'(\eta) \rightarrow 0, \quad \theta_i(\eta) \rightarrow 0, \quad \text{as } \eta \rightarrow \infty, \end{aligned} \quad (20)$$

for $i \geq 0$, where δ_{ij} is the Kronecker delta, which is defined by

$$\delta_{ij} = \begin{cases} 1 & \text{if } i = j \\ 0 & \text{if } i \neq j. \end{cases} \quad (21)$$

The skin-friction coefficient and the local Nusselt number (14) are given now by

$$\begin{aligned} \frac{1}{2}C_f \text{Re}_x^{1/2} &= \frac{1}{\sqrt{2}}f''(0) \approx \frac{1}{\sqrt{2}}\sum_{i=0}^4 f_i''(0)M^i, \\ \text{Nu}_x/\text{Re}_x^{1/2} &= -\frac{1}{\sqrt{2}}\theta'(0) \approx -\frac{1}{\sqrt{2}}\sum_{i=0}^4 \theta_i'(0)M^i, \end{aligned} \quad (22)$$

for $M \ll 1$.

3.3 Asymptotic solution for large M

In order to study the case when $M \gg 1$, we introduce the following new variables; see [22],

$$F(z) = M^{1/2}f(\eta), \quad \phi(z) = \theta(\eta), \quad z = M^{1/2}\eta. \quad (23)$$

Equations 9 and 10 then become

$$F''' - 2F' + \epsilon \left[(n-1)FF'' - 2nF'^2 \right] = 0, \quad (24)$$

$$\frac{1}{Pr} \phi'' + \epsilon [(n - 1)F\phi' - 2mF'\phi] = 0, \tag{25}$$

subject to the boundary conditions

$$\begin{aligned} F(0) = 0, \quad F'(0) = 1, \quad \phi(0) = 1, \\ F'(\infty) \rightarrow 0, \quad \phi(\infty) \rightarrow 0, \end{aligned} \tag{26}$$

where $\epsilon = 1/M \ll 1$ and now primes denote differentiation with respect to z . Because ϵ is small, we can look for a solution of Eqs. 24 and 25 of the following form:

$$F(z) = \sum_{i=0}^{\infty} F_i(z)\epsilon^i, \quad \phi(z) = \sum_{i=0}^{\infty} \phi_i(z)\epsilon^i. \tag{27}$$

Substituting (27) in Eqs. 24 and 25, we get for the functions $F_0(z)$ and $\phi_0(z)$ the following differential equations:

$$\begin{aligned} F_0''' - 2F_0' = 0, \quad \phi_0'' = 0, \\ F_0(0) = 0, \quad F_0'(0) = 1, \quad \phi_0'(0) = 0, \\ F_0'(\infty) \rightarrow 0, \quad \phi_0(\infty) \rightarrow 0. \end{aligned} \tag{28}$$

We notice from these equations that $\phi_0(z)$ does not satisfy the corresponding boundary conditions. Therefore, the problem of thermal field is a singular one for very large values of M . Further, we have

$$\begin{aligned} F_i''' - 2F_i' + (n - 1) \sum_{j=0}^{i-1} F_j F_{i-j-1}'' - 2n \sum_{j=0}^{i-1} F_j' F_{i-j-1}' = 0, \\ F_i(0) = 0, \quad F_i'(0) = 0, \quad F_i'(\infty) \rightarrow 0, \end{aligned} \tag{29}$$

for $i \geq 1$. The skin-friction coefficient (14) is given now by

$$\frac{1}{2} C_f Re_x^{1/2} = \frac{1}{\sqrt{2}} f''(0) \approx \sqrt{M} \sum_{i=0}^4 F_i''(0) M^{-i}, \tag{30}$$

for $M \gg 1$.

4 Results, discussion and conclusions

Equations 9 and 10 subject to the boundary conditions (11) have been solved numerically for several values of the velocity power index n and the magnetic parameter M , using the Keller-box method as described in [20]. For convenience and space conservation, the Prandtl number Pr and the temperature power index m are fixed, namely $Pr = 7$ (such as water) and $m = 10$. We consider various variations of n , namely $0 < n < 1, n > 1, n = 1/3, n = 1$ and $n = -1$.

4.1 $0 < n < 1$

As concluded by Kuiken [15], for this case, the solution is valid far enough upstream ($x \rightarrow -\infty$) where the condition $v/(u_s|x|) \ll 1$ applies. This condition was discussed in [15]. The values of $f''(0)$ are given in Table 1 for some values of n . The values obtained by Kuiken [15] using the series method are also included in this table. It is seen that the numerical values for $M = 0$ (magnetic field is absent) obtained by using the present method are exactly the same as given by Kuiken [15] for all values of n considered. The velocity and temperature profiles for different values of n when $M = 1$ are presented in Figs. 1 and 2, respectively. The velocity profiles were not given in [15], thus no comparison can be made. These figures show that the boundary conditions are satisfied, which supports the validity of the present results. It is seen from Fig. 1 that the velocity boundary-layer thickness decreases slightly

Table 1 Values of $f''(0)$ when $0 < n < 1$

n	$M = 0$		$M = 1$	$M = 2$
	Kuiken [15]	Present results		
0.2	-0.38191349	-0.3819	-1.4191	-2.0017
0.4	-0.63898882	-0.6390	-1.5310	-2.0830
0.6	-0.83961231	-0.8396	-1.6352	-2.1612
0.8	-1.00779210	-1.0078	-1.7331	-2.2365

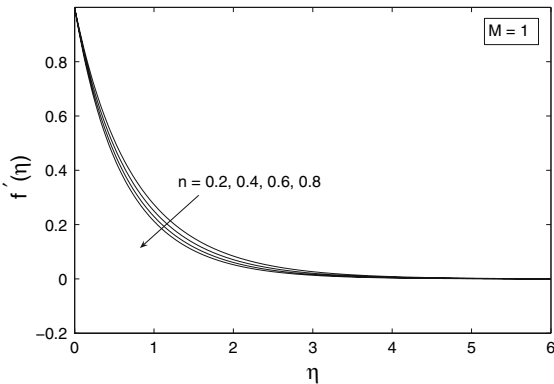


Fig. 1 Velocity profiles for different values of n ($0 < n < 1$) when $M = 1$

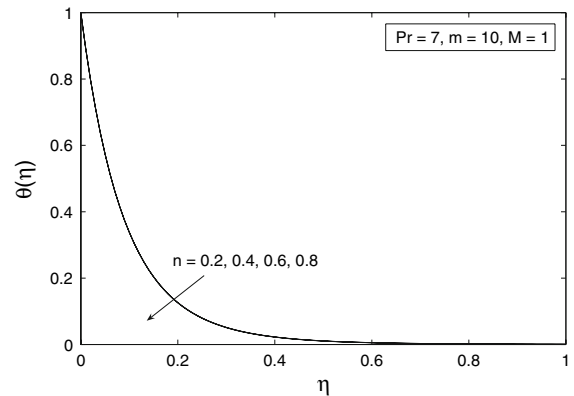


Fig. 2 Temperature profiles for different values of n ($0 < n < 1$) when $Pr = 7, m = 10$ and $M = 1$

with an increase in n , which in turn increases the velocity gradient at the surface. Thus, the absolute value of the skin-friction coefficient $|f''(0)|$ increases with increasing of n . This observation is in agreement with the values of $f''(0)$ given in Table 1. The same feature is observed for the effect of n on the temperature profiles, but the effect of n on the velocity profiles is much more pronounced than on the temperature profiles. Further, the values of $f''(0)$ as shown in Table 1 are negatives, which mean that the sheet exerts a drag force on the fluid.

4.2 $n > 1$

For $n > 1$, the solution is valid close enough to $x = 0$ as soon as $v/(u_s|x|) \ll 1$ applies. Table 2 presents the values of $f''(0)n^{-1/2}$ for $M = 0$ and different values of n , as considered in [15]. Again, in this table, we compare our results with those reported in [15], and they show a very good agreement. In addition, we found two solutions for moderate and large values of n . This result is new and was not reported in [15]. The velocity and temperature profiles, which support the dual nature of the solution, are presented in Figs. 3 and 4, respectively. Figure 3 shows that the second solution has a region of reversed flow (has $f'(\eta) < 0$) located away from the plate. These profiles also satisfy the boundary conditions (11), thus should not be neglected. Figure 4 shows a monotonically decreasing manner of the temperature profiles as η increases (one moves away from the plate). The temperature profiles for the first and the second solutions do not show much different, compared to those of velocity. Moreover, the boundary-layer thickness decreases as n increases, which in turn increases the temperature gradient at the surface, hence increases the heat-transfer rate there.

The velocity and temperature profiles for $n = 2$ and different values of M are presented in Figs. 5 and 6, respectively. It is seen that the velocity gradient at the surface increases but the temperature gradient decreases as M increases. Thus, introducing M will increase the skin friction but decrease the heat-transfer rate at the surface. However, the effect of M on the thermal field is less pronounced compared to the flow field. This effect becomes

Table 2 Values of $f''(0)n^{-1/2}$ for different values of n when $M = 0$

n	Kuiken [15]	Present results	
		First solution	Second solution
1.5	-1.19485513	-1.1949	
2	-1.21601870	-1.2160	
2.5	-1.22896403	-1.2290	
3	-1.23767321	-1.2377	
4	-1.24863030	-1.2486	-1.2548
5	-1.25523518	-1.2552	-1.2621
10	-1.26849732	-1.2685	-1.2768
100	-1.28047587	-1.2805	-1.2902
1000	-1.28167528	-1.2817	-1.2915

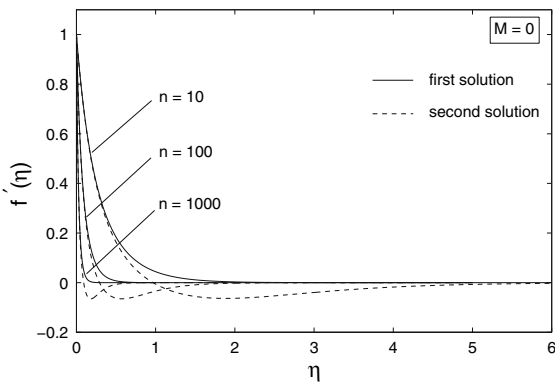


Fig. 3 Velocity profiles for $n = 10, 100$ and $1,000$ when $M = 0$

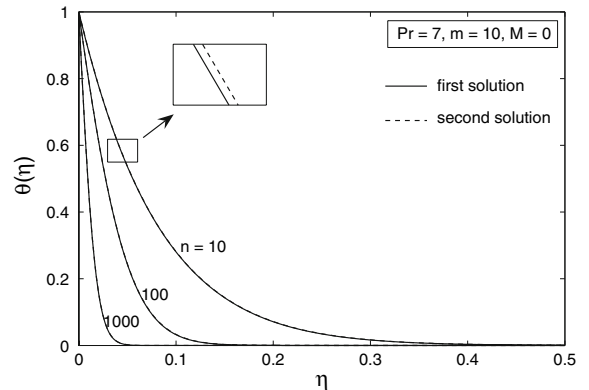


Fig. 4 Temperature profiles for $n = 10, 100$ and $1,000$ when $Pr = 7, m = 10$ and $M = 0$

less important for larger values of n , for example when $n = 1,000$, as shown in Fig. 7. As mentioned previously, the second solution can be determined for this value of n . The temperature profiles for this case are not presented here since they show not much difference between the first and second solutions as well as for different values of M .

The values of the skin-friction coefficient $f''(0)$ and the local Nusselt number $-\theta'(0)$ are also obtained by using series expansion (22) for small values of M , and the series expansion (30) for large values of M , besides using the direct numerical computation given by (14). For $Pr = 7, m = 10$ and $n = 10$, Equation 22 becomes

$$\begin{aligned} \frac{1}{2}C_f Re_x^{1/2} &\approx (-4.0113 - 0.2552M + 0.0096M^2 - 0.0011M^3 + 0.0002M^4), \\ Nu_x/Re_x^{1/2} &\approx (-12.2194 + 0.0673M - 0.0025M^2 + 0.0003M^3 - 0.0001M^4), \end{aligned} \tag{31}$$

while for $n = 10$, Eq. 30 becomes

$$\frac{1}{2}C_f Re_x^{1/2} \approx \sqrt{M}(-1.4142 - 5.7688M^{-1} + 12.2727M^{-2} + 30.9766M^{-3} - 1.4606M^{-4}). \tag{32}$$

These values of $f''(0)$ and $-\theta'(0)$ are presented in Tables 3 and 4, while the variations with M are presented in Figs. 8 and 9, respectively. It is observed that there is a good agreement between numerical solutions of the full equations and the solutions for small and large values of M . We are, therefore, able to determine the values of $f''(0)$ for all values of M , i.e., $0 < M < +\infty$. However, it is not possible to determine the values of $-\theta'(0)$ for all values of M due to its singular behaviour for large values of M .

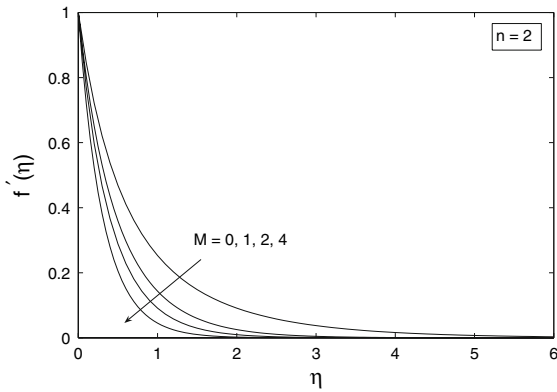


Fig. 5 Velocity profiles for $M = 0, 1, 2$ and 4 when $n = 2$

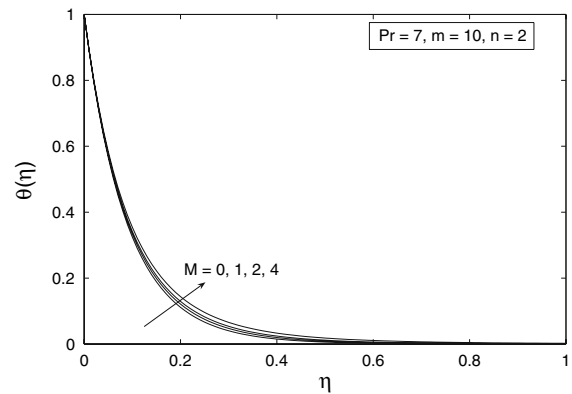


Fig. 6 Temperature profiles for $M = 0, 1, 2$ and 4 when $Pr = 7, m = 10$ and $n = 2$

Table 3 Values of $f''(0)$ when $n = 10$ (for the first solution)

M	Numerical, Eq. 14	Small M , Eq. 22	Large M , Eq. 30
0	-4.0113	-4.0113	
0.1	-4.0368	-4.0368	
0.2	-4.0620	-4.0620	
0.3	-4.0871	-4.0871	
0.4	-4.1120	-4.1119	
0.5	-4.1367	-4.1366	
1	-4.2580		
2	-4.4898		
4	-4.9188		
10	-6.0206		
100	-14.7078		-14.7064
1000	-44.9036		-44.9034
10000	-141.4790		-141.4790

Table 4 Values of $-\theta'(0)$ when $Pr = 7, m = 10$ and $n = 10$ (for the first solution)

M	Numerical, Eq. 14	Small M , Eq. 22
0	12.2194	12.2194
0.1	12.2127	12.2127
0.2	12.2060	12.2060
0.3	12.1993	12.1994
0.4	12.1927	12.1929
0.5	12.1862	12.1864
1	12.1540	
2	12.0923	
4	11.9776	
10	11.6791	
100	9.2117	
1000	4.2512	
10000	-	

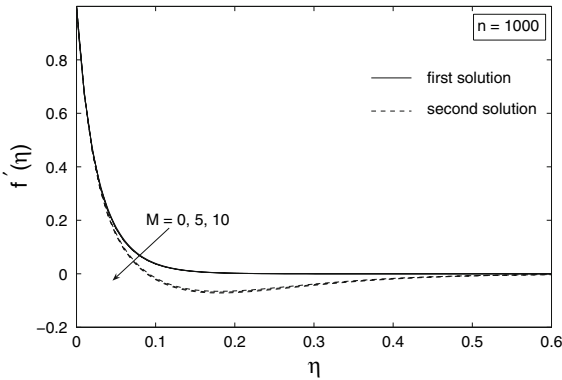


Fig. 7 Velocity profiles for $M = 0, 5$ and 10 when $n = 1,000$

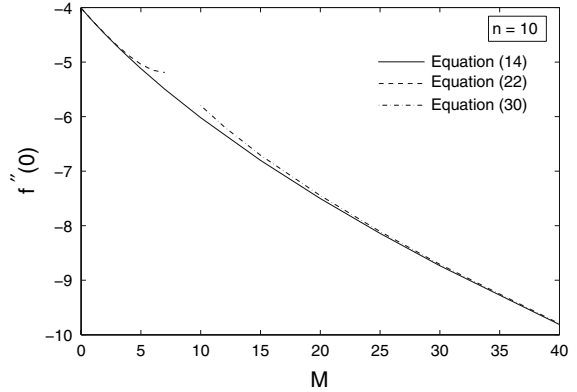


Fig. 8 Variation of $f''(0)$ with M when $n = 10$

4.3 $n = 1/3$

We notice that in this case, a first integral of Eq. 9 does exist also for $M \neq 0$, that is

$$f'' - \frac{2}{3} f f'' - 2Mf = f''(0). \tag{33}$$

Assuming that $f'(\eta)$ decreases exponentially as $\eta \rightarrow \infty$, Eq. 33 gives

$$-2Mf(\infty) = f''(0). \tag{34}$$

Therefore, if $f'(\eta)$ decreases exponentially as $\eta \rightarrow \infty$, then $f(\infty)$ should be finite when $M \neq 0$. Let us assume that there would be (as in Kuiken’s [15] case for $M = 0$) solutions $f'(\eta)$ which decrease algebraically when $\eta \rightarrow \infty$, that is

$$f'(\eta) = a\eta^{-b} \quad \text{as } \eta \rightarrow \infty, \tag{35}$$

where a and b are constants with $b > 0$ and $b \neq 1$. In this case, we have

$$f(\eta) = K + \frac{a}{1-b} \eta^{1-b}, \tag{36}$$

and Eq. 34 becomes

$$-\frac{2}{3} \frac{a}{1-b} \eta^{1-2b} - 2M \left(K + \frac{a}{1-b} \eta^{1-b} \right) = f''(0) \quad \text{as } \eta \rightarrow \infty. \tag{37}$$

This asymptotic equation can be satisfied only for $b = 1/2$ and when $M = 0$ [15]. However, it cannot be satisfied when $M \neq 0$ and the present problem does not admit algebraic solutions of Kuiken’s [15] type, which decrease asymptotically.

4.4 $n = 1$

The velocity and temperature profiles for different values of M are presented in Figs. 10 and 11, respectively. It is seen that the velocity boundary-layer thickness decreases whereas the thermal boundary-layer thickness increases with an increase in M . Thus, the skin-friction coefficient increases but the rate of heat transfer at the surface decreases as M increases. These results are consistent with the results for both cases of $0 < n < 1$ and $n > 1$. Therefore, it can be concluded that the solution for the case of $n = 1$ is a valid approximation for all $x < 0$ as long as $v/(u_s|x|) \ll 1$ applies.

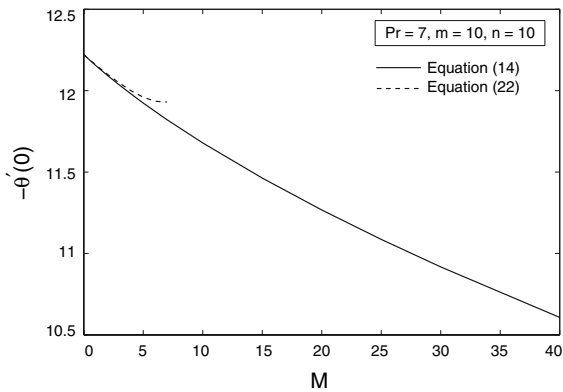


Fig. 9 Variation of $-\theta'(0)$ with M when $Pr = 7, m = 10$ and $n = 10$

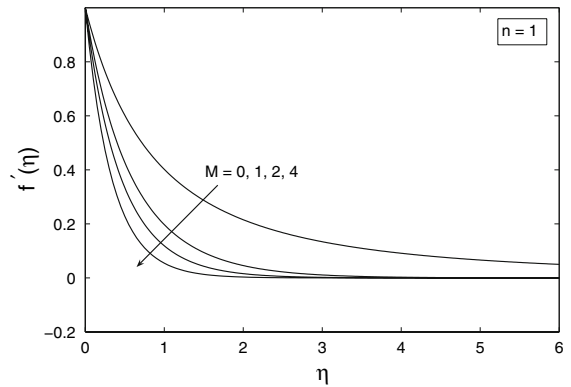


Fig. 10 Velocity profiles for different values of M when $n = 1$

Fig. 11 Temperature profiles for different values of M when $Pr = 7, m = 10$ and $n = 1$

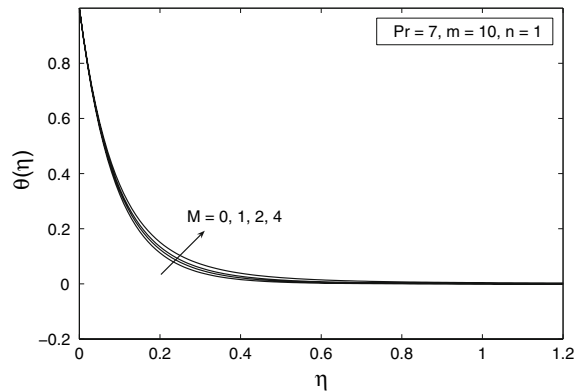


Table 5 Values of $f''(0)$ for $n = 1$

M	Eq. 9	Eq. 39
0	-1.1547	-1.1547
1	-1.8257	-1.8257
10	-4.6188	-4.6188
100	-14.1892	-14.1892
1000	-44.7363	-44.7363
10000	-141.4261	-141.4261

The case $n = 1$ is also a “friendly” case, since the momentum equation (9) admits the first integral

$$f''^2 = 2M f'^2 + \frac{4}{3} f'^3. \tag{38}$$

This equation yields for the wall shear stress the (valuable) exact result

$$f''(0) = -\sqrt{2M + \frac{4}{3}}, \tag{39}$$

for $n = 1$. Table 5 presents some results for $f''(0)$ obtained by direct numerical solution of Eq. 9 and using relation (39) for some values of M when $n = 1$. It is seen that the agreement is excellent. Therefore, this special case could also serve as a benchmark, both for the analytical and numerical investigations of the problem.

$$4.5 \quad n = -1$$

In this case Eq. 9 has the exact analytical solution

$$f(\eta) = \frac{1 - e^{-\sqrt{2(M-1)}\eta}}{\sqrt{2(M-1)}}, \quad (40)$$

for $M > 1$. It should be mentioned that for $n = -1$ the applied magnetic field given by Eq. 7 is constant.

Acknowledgements The authors wish to express their very sincere thanks to the reviewers for their valuable comments and suggestions. Special thanks also goes to Dr. E. Magyari who has very kindly helped us to improve the paper. This work is supported by a research grant (SAGA fund: STGL-013-2006) from the Academy of Sciences Malaysia.

References

1. Sakiadis BC (1961) Boundary layer behavior on continuous solid surfaces: I. The boundary layer equations for two-dimensional and axisymmetric flow. *AIChE J* 7:26–28
2. Sakiadis BC (1961) Boundary-layer behavior on continuous solid surfaces: II. The boundary-layer on a continuous flat surface. *AIChE J* 7:221–225
3. Gupta PS, Gupta AS (1977) Heat and mass transfer on a stretching sheet with suction and blowing. *Can J Chem Engng* 55:744–746
4. Dutta BK, Roy P, Gupta AS (1985) Temperature field in flow over a stretching sheet with uniform heat flux. *Int Commun Heat Mass Transfer* 12:89–94
5. Grubka LJ, Bobba KM (1985) Heat transfer characteristics of a continuous stretching surface with variable temperature. *Trans ASME J Heat Transfer* 107:248–250
6. Kumari M, Takhar HS, Nath G (1990) MHD flow and heat transfer over a stretching surface with prescribed wall temperature or heat flux. *Wärme- und Stoffübertr* 25:331–336
7. Liao S-J, Pop I (2004) On explicit analytic solutions of boundary-layer equations about flows in a porous medium or for a stretching wall. *Int J Heat Mass Transfer* 47:75–85
8. Nazar R, Amin N, Filip D, Pop I (2004) Unsteady boundary layer flow in the region of the stagnation point on a stretching sheet. *Int J Engng Sci* 42:1241–1253
9. Crane LJ (1970) Flow past a stretching plate. *J Appl Math Phys (ZAMP)* 21:645–647
10. Banks WHH (1983) Similarity solution of the boundary layer equations for a stretching wall. *J Mech Theor Appl* 2:375–392
11. Magyari E, Keller B (1999) Heat and mass transfer in the boundary layers on an exponentially stretching continuous surface. *J Phys D: Appl Phys* 32:577–585
12. Magyari E, Keller B (2000) Exact solutions for self-similar boundary-layer flows induced by permeable stretching surfaces. *Eur J Mech B-Fluids* 19:109–122
13. Magyari E, Ali ME, Keller B (2001) Heat and mass transfer characteristics of the self-similar boundary-layer flows induced by continuous surfaces stretched with rapidly decreasing velocities. *Heat Mass Transfer* 38:65–74
14. Carragher P, Crane LJ (1982) Heat transfer on a continuous stretching sheet. *J Appl Math Mech (ZAMM)* 62:564–565
15. Kuiken HK (1981) On boundary layers in fluid mechanics that decay algebraically along stretches of wall that are not vanishingly small. *IMA J Appl Math* 27:387–405
16. Shercliff JA (1965) *A textbook of magnetohydrodynamic*. Oxford Pergamon Press
17. Cobble MH (1977) Magnetohydrodynamic flow with a pressure gradient and fluid injection. *J Eng Math* 11:249–256
18. Cobble MH (1980) Magnetohydrodynamic flow for a non-Newtonian power-law fluid having a pressure gradient and fluid injection. *J Eng Math* 14:47–55
19. Helmy KA (1994) Solution of the boundary layer equation for a power law fluid in magneto-hydrodynamics. *Acta Mech* 102:25–37
20. Cebeci T, Bradshaw P (1988) *Physical and computational aspects of convective heat transfer*. Springer, New York
21. Ariel PD (1994) Hiemenz flow in hydromagnetics. *Acta Mech* 103:31–43
22. Chiam TC (1995) Hydromagnetic flow over a surface stretching with a power-law velocity. *Int J Engng Sci* 33:429–435